Critical Roles of Ultrafast Energy Funnelling and Ultrafast Singlet-Triplet Annihilation in Quasi-Two-Dimensional Perovskite Optical Gain Mechanisms

Isabella Wagner[1,2], Wouter T.M. Van Gompel[3], Laurence Lutsen[3,4], Dirk Vanderzande[3,4], Chern Chuang[5], Sheng Hsiung Chang[6], Paul A. Hume[1,2], Michael B. Price[1,2], Pieter Geiregat[7,8], Justin M. Hodgkiss[1,2]* and Kai Chen[1,9,10]*

[1] MacDiarmid Institute for Advanced Materials and Nanotechnology, New Zealand

[2] School of Chemical and Physical Sciences, Victoria University of Wellington, 6012, Wellington, New Zealand

[3] Hybrid Materials Design (HyMaD), Institute for Materials Research (IMO), Hasselt University, 3500, Hasselt, Belgium

[4] Associated Laboratory IMOMEC, Imec, Wetenschapspark 1, 3590, Diepenbeek, Belgium

[5] Department of Chemistry and Biochemistry, University of Nevada, 4505 S Maryland Pkwy, Las Vegas, Nevada 89154, United States

[6] Department of Physics, Chung Yuan Christian University, 320314, Taoyuan, Taiwan

[7] Physics and Chemistry of Nanostructures, Ghent University, 9000, Ghent, Belgium

[8] Center for Nano and Biophotonics, Ghent University, Belgium

[9] The Dodd-Walls Centre for Photonic and Quantum Technologies, Dunedin, New Zealand

[10] Robinson Research Institute, Victoria University of Wellington, 6012, Wellington, New Zealand

*Correspondence should be sent to K. C. (Kai.Chen@vuw.ac.nz) and J.M.H. (Justin.Hodgkiss@vuw.ac.nz)

Abstract

Quasi-two-dimensional (Q2D) perovskites possess considerable potential for light emission and amplification technologies. Recently, mixed films containing Q2D perovskite grains with varying layer thicknesses have shown great promise as carrier concentrators, effectively mitigating trap-mediated recombination. In this strategy, photo-excitations are rapidly funnelled down an energy gradient to the thickest grains, leading to amplified spontaneous emission (ASE). However, the quantum confined Q2D slabs also stabilize the formation of unwanted triplet excitons, resulting in parasitic quenching of emissive singlet states. Here, we use a novel ultrafast photoluminescence spectroscopy to study photoexcitation dynamics in mixed layer Q2D perovskites. By analysing spectra with high temporal and energy resolution, we find that sub-picosecond energy transfer to ASE sites is accompanied by excitation losses due to triplet formation on grains with small and intermediate thicknesses. Further accumulation of triplets creates a bottleneck in the energy cascade, effectively quenching incoming singlet excitons. This ultrafast annihilation within 200 fs outpaces energy transfer to ASE sites, preventing the build-up of population inversion. Our study highlights the significance of investigating photoexcitation dynamics on ultrafast timescales, encompassing lasing dynamics, energy transfer, and singlet-triplet annihilation, to gain crucial insights into the photophysics of the optical gain process in Q2D perovskites.

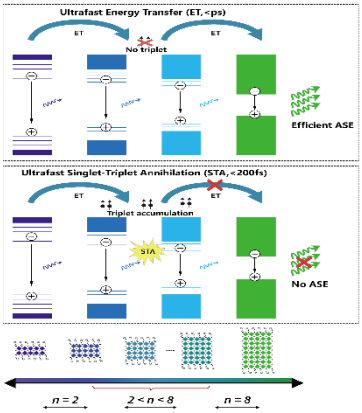

Table of Contents figure

Ultrafast broadband photoluminescence spectroscopy provides insights into the lasing dynamics, energy transfer, and singlet-triplet annihilation in mixed-layer quasi-two-dimensional perovskites. Rapid energy funnelling to the sites of amplified spontaneous emission occurs within sub-picosecond timescales. However, the accumulation of triplet excitons effectively quenches incoming singlet excitons, creating a bottleneck in the energy cascade and hindering the development of population inversion.

Metal halide perovskite semiconductors have emerged as promising candidates for optoelectronic applications like solar harvesting [1,2], light-emitting diodes (LEDs) [3,4], and semiconductor lasers [5,65,6] due to their excellent optoelectronic properties, including their high absorption coefficient [77], bright photoluminescence [8], high carrier mobility [9,10], and tunable bandgap [11,12]. More recently interest in nanostructures has grown, especially in mixed layered quasi-two-dimensional (Q2D) hybrid organic-inorganic perovskites because of their improved stability compared to bulk materials and ability to act as carrier concentrator [3,13–16].

In Q2D perovskites, <*n*> layers of metal halide octahedra are sandwiched between a bilayer of a bulky organic spacer, like phenethylammonium (PEA), which acts as an insulating barrier. This provides better resistance against humidity and light irradiation compared to their 3D counterparts [17–20] and results in clear size- and dielectric-confinement effects [21,22]. The high excitonic character of small-<*n*> Q2D domains has been associated with an increased radiative recombination probability and a rapid energy transfer cascade from wide to small bandgap domains [16,23] (see Figure 1a): this may outpace trapping on defect states and result in high photoluminescence quantum yields. High-efficiency perovskite LEDs [3,24] have been achieved with this approach, but an efficiency roll-off at higher current densities impedes their commercialization [25,26]. This concept of carrier concentration also facilitates the build-up of population inversion and has been exploited in the design of Q2D perovskites as optical gain media for low threshold lasing [27–30]. However, the use of mixed Q2D perovskite films in lasing applications has been less successful than for LEDs.

Confinement effects can also impact the splitting of the exciton fine structure. The enhanced overlap between the electron and hole wavefunctions increases the exchange energy, resulting in increased singlet-triplet energy splitting [31–33]. Although there is an ongoing debate about the exciton fine structure splitting in layered perovskites [34–36], experimental observations point to a low lying dark (triplet) state in highly confined Q2D perovskites [37–41]. While their radiative recombination is spin-forbidden, these dark states possess complex excited state pathways. Depending on the extent of the

energy level splitting, it is possible that nonradiative recombination and reverse intersystem crossing (RISC) back to the bright state occurs. Triplet excitons may also interact with the singlet population by quenching them via singlet-triplet annihilation (STA). Although this interaction is the major limitation preventing continuous wave (CW) and direct current injection lasing within organic semiconductors [42–44], little attention has been given to the presence of triplet excitons within mixed Q2D perovskite films.

Qin *et al*. [5,45] stressed the importance of triplet state management in Q2D perovskites for efficient LED and lasing applications. They reported that the rapid diminishing of the amplified spontaneous emission (ASE) signal under pulsed excitation in the absence of a triplet quenching species results in the lasing death phenomenon in perovskite semiconductors [5]. However, other reports present inconsistent observations about ASE stabilities and the involvement of inorganic triplet states in lasing degradation. Specifically, a recent study reported stable ASE evolution under pumped excitation with and without the presence of a triplet quencher [46]. Although this study also reported a long-lived photoluminescence (PL) feature associated with RISC from the presence of triplet states, no effect was observed on the ASE stability [46].

The evidence suggests that triplet states in Q2D films control the radiative recombination that is crucial for the design of LEDs and lasers. However, there have been few investigations on the interactions between singlet states and accumulated triplet excitons in Q2D perovskites [45–47]. Since these states are not directly generated by photoexcitation and their detectable optical signatures are expected to be weak or overlapped with other features at room temperature [48], it is challenging to investigate singlet-triplet interactions on relevant ultrafast timescales using common optical spectroscopy methods. To date, mostly ill-defined triplet sensitizers have been used to track the presence of triplet populations indirectly [5,40,49].

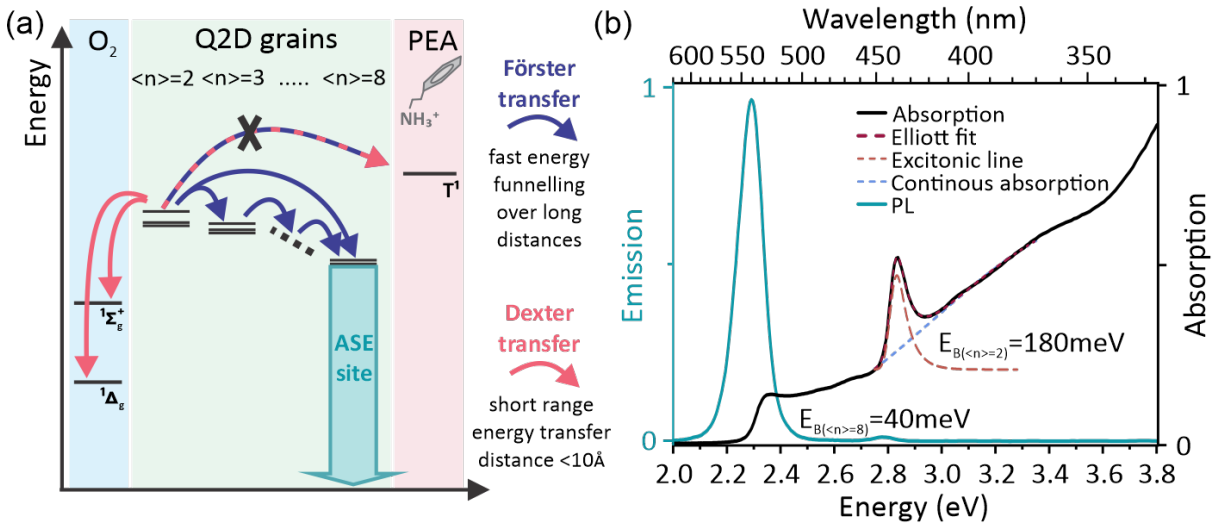

Figure 1: Schematic illustration of energy transfer between energy levels within perovskite grains with a different inorganic layer thickness (<n>), attached organic ligands, and molecular oxygen. (b) Steady-state absorption and emission spectrum of the mixed Q2D perovskite film with corresponding exciton binding energies extracted from Elliott fitting and temperature-dependent PL experiments (SI Figure S1) for <n> = 2 and <n> = 8 grains, respectively.

In this investigation, we utilized broadband transient photoluminescence (PL) facilitated by transient grating PL spectroscopy to achieve exceptional energy and temporal resolution, enabling a comprehensive examination of photoexcitation dynamics.[50] By manipulating the photoexcitation repetition rate as an experimental parameter, we were able to regulate the concentration of accumulated triplet excitons, thereby facilitating an in-depth analysis of the interplay between singlet energy funneling and singlet-triplet annihilation processes occurring on ultrafast timescales. This unique method is used to determine the role of out-of-plane confinement on the triplet exciton stabilisation in Q2D domains, and the mechanism by which accumulation of long-lived triplet states in highly excitonic Q2D perovskite grains impedes population inversion in mixed Q2D perovskite films.

Results

To control the accumulation of triplet states and investigate the effect of out-of-plane confinement and energy transfer dynamics on ASE performance, we selected a system of mixed layered

phenethylammonium (PEA) formamidinium (FA) lead bromide perovskites, $PEA_2FA_{n-1}Pb_nBr_{3n+1}$, where <*n*> describes the number of inorganic sheets, composed of corner-sharing $PbBr_6^{4-}$ octahedra, sandwiched between bilayers of the large organic PEA cations. A 90 nm thick film was fabricated by spin-coating the precursor solution onto a quartz substrate, using anti-solvent dripping with toluene during spinning, followed by annealing at 70 °C for 15 min and 100 °C for 5 min on a hotplate in a glovebox (see Supporting Information (SI) for details).

The absorption and emission properties of layered perovskites depend on the thickness <*n*> of the inorganic layer [51,52]. Figure 1b reveals that the film consists of a mixture of Q2D perovskite slabs with different layer thicknesses <*n*>. While the absorption onset at around 2.1 eV originates from perovskite emitters with mainly <*n*> = 8 [45], the sharp peak at 2.8 eV is characteristic of highly confined slabs with a thickness of <*n*> = 2 [51]. The emission peaks in the temperature-dependent photoluminescence spectra in SI Figure S1 confirm that the Q2D film consists of a mixture of perovskite slabs with layers of various thicknesses.

The effect of long-lived dark states on the ASE performance of the Q2D perovskite film was investigated using oxygen to control the ability to accumulate inorganic triplet states. At 3.3 eV, the triplet energy level of the organic ligand PEA is well above the perovskite bandgap [45] (see Figure 1a). Rather than function as an inorganic triplet state quencher, the organic ligand confines triplets within the perovskite domains. Conversely, the two low-lying singlet excited states of oxygen [53] and its exceptional diffusion through the Q2D perovskite matrix [54] indicate oxygen efficiently quenches triplet states. Hence, by placing the perovskite film into an air-tight sample holder, a switch between accumulating inorganic triplet states and triplet exciton-free conditions is achieved by applying a vacuum or flooding the sample chamber with ambient air, respectively. The tunable and high repetition rate of the laser system is then used to progressively mimic continuous wave pumping conditions to directly study the impact of accumulated triplet excitons on ASE performance.

the findings of Qin *et al*. [5].

Figure 2c and 2d shows the ultrafast PL spectra of Q2D thin film excited at 343 nm above the ASE threshold. In the presence of oxygen condition (Fig 2c), we clearly observe a rapid spectral narrowing, the signature of ASE formation. The outstanding lasing character of the Q2D PVSK can be related to the < 2 picosecond (ps) ASE formation time for rapid, dynamic lasing threshold attainment. On the other hand, under vacuum conditions, without oxygen as a triplet quencher, the ultrafast PL spectra under 343 nm excitation lacks the signature of ASE formation (Fig 2d). Considering that the presence of triplet excitons strongly impedes ASE, our observation suggests that the critical time scale of STA must be in the sub-picosecond to few picoseconds range, a previously unexplored temporal window for STA dynamics.

In Figures 2c and 2d, the transient PL spectra of samples in the presence and absence of an oxygen environment also show a common feature of a short lived, hot emission. The peak at 2.8 eV of the hot PL spectra is consistent with the PL spectrum of the <*n*>=2 nanoplate, and the main contribution of the transient PL between 2.5 and 2.6 eV is likely to come from the nanoplate with different thicknesses between <*n*>=3 and <*n*>=5. Therefore, we can assign the short-lived hot emission as the signature of energy funnelling in the mixed-grain Q2D PVSK.[23]

So far, our experimental results highlight that, under high-fluence excitation conditions, the sub-to-few picoseconds timescale is critical for understanding the interplay of ASE, energy funnelling, and STA and how they manifest in the lasing dynamics of Q2D PVSK. To verify the relationship between ASE, STA, and energy funnelling, we use 515 nm excitation to selectively excite the <*n*>=8 plates and bypass the energy funnelling.

Figure 2: Steady-state PL spectrum above (red; $n_c = 30 \cdot 1018\ cm^{-3}$) and below (green; $n_c = 1{\cdot}10^{18}\ cm^{-3}$) the ASE threshold in the presence of oxygen and without, excited with a photon energy of (a) 3.6 eV and (b) 2.4 eV at a laser repetition rate of 58 kHz. (c) The ultrafast PL spectral maps after photoexcitation at 3.6 eV under O_2 environment (c) and vacuum (d) at a laser repetition rate of 58 kHz.

In contrast to experiments carried out by Qin *et al.* [55], we also selectively excited only the thicker (higher <*n*>) grains of the Q2D perovskite film using a photon energy of 2.4 eV (515 nm, <130 fs, 58 kHz) while recording steady-state PL spectra under the conditions indicated in Figure 2b. Below the ASE threshold, the broadband spectrum around 2.3 eV in Figure 2b is similar to the spectrum after excitation with higher photon energy. The stable ASE peak which appears above the ASE threshold, irrespective of the presence of an inorganic triplet quencher, is evidence that triplets do not play a role when only the high-<*n*> grains of the perovskite films are excited. This finding also precludes oxygen's role as a quencher for photoexcited species beyond triplet quenching.

Next, we aim to directly quantify the interactions between singlet and long-lived triplet excitons on ultrafast timescales to determine whether triplet states quench singlets before they can transfer to grains with lower bandgaps and therefore entice ultrafast singlet-triplet annihilation (STA) pathways. It is a fundamental challenge to study STA dynamics via conventional ultrafast spectroscopy because singlet and triplet populations are each time-dependent and coupled to each other via intersystem crossing as well as STA. Here, we employ a new ultrafast PL spectroscopy technique based on a high repetition fibre laser amplifier with an integrated pulse picker in order to control the accumulated triplet exciton concentration within the perovskite slabs by tuning the time interval between arriving laser pulses, i.e., the laser repetition rate, as illustrated in Figure 3a. In the case of a low laser repetition rate, there is sufficient time between excitation pulses for the triplet states to decay before the next excitation pulse arrives. Consequently, STA should not be present, and the build-up of a similar singlet state population on the ASE site is therefore possible. A shorter time interval between successive laser pulses (Figure 3a (II)) allows a fraction of the inorganic triplet population to still be present when the next laser pulse creates excitations. This accumulated long-lived triplet population may interact with the newly generated singlet excitons via STA, effectively quenching the singlet state population and leaving behind a triplet exciton in a higher excited state. Hence, an even shorter time interval between

single excitation pulses (Figure 3a (III)) allows the even greater accumulation of the triplet states, which then interact with the newly injected singlet population of the following excitation pulse. Moreover, this approach allows us to investigate STA dynamics similar to optical and electrical pump operation conditions.

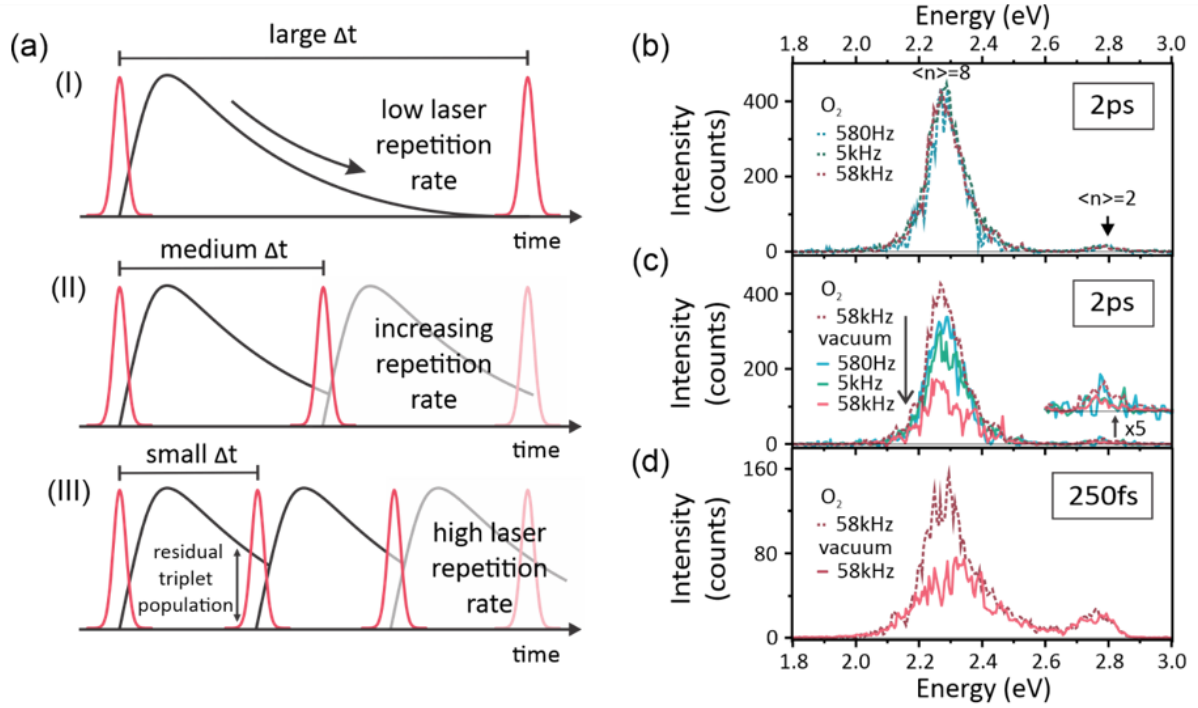

Figure 3: (a) Schematic illustration of laser repetition rate-dependent triplet state accumulation. (I) For a low laser repetition rate, the long-lived dark states decay until the next laser pulse arrives to excite the sample again. (II-III) A decreasing laser pulse period prevents the full relaxation of the excited inorganic triplet state population until the next laser pulse excites the perovskite film again. (b) Repetition rate-dependent transient PL spectra at 2 ps after photoexcitation (3.6 eV, $n_c = 1.9 \cdot 10^{18}$ cm^{-3}) in the presence of oxygen and (c) under vacuum. (d) Comparison of PL spectra at 250 fs after excitation recorded in the presence and absence of oxygen using a high laser repetition rate.

In Figures 3b, 3c, and 3d, we measure the transient PL spectra under different laser repetition rates and with/without an oxygen environment. Because the measured sample spot and excitation conditions are the same, the transient PL intensities can be directly compared. The PL spectrum at 2 ps after photoexcitation was monitored to determine the repetition rate-dependent quenching behaviour, a time point where the PL intensity build-up on the ASE site reaches its maximum (see SI

Figure S5). As shown in Figure 3b, the overall emission intensity of the Q2D perovskite film under an ambient atmosphere is unaffected by the laser repetition rate in the presence of oxygen. However, the PL intensity of the perovskite film stored in an oxygen-free environment (see Figure 3c) is much lower when recorded with a high laser repetition rate (58 kHz) and steadily recovers as the laser repetition rate decreases. Since this lower repetition rate corresponds to a longer time interval between successive laser pulses, the amount of accumulated long-lived triplet states decreases, as does the probability of STA. At a low laser repetition rate of only 580 Hz, the emission intensity for both conditions can barely be distinguished, suggesting that energy funnelling is not hampered through the presence of accumulated triplet states. Since ASE can be observed under vacuum conditions with a low repetition rate and threshold carrier densities, like those in an oxygen-containing environment (see SI Figure S3), we conclude that most triplet excitons had recombined before the re-excitation of the perovskite film.

So far, we found two features of ASE in Q2D PVSK: first, the existence of triplet excitons can completely prohibit ASE. Second, the onset of ASE is within the early picosecond timescale after photoexcitation. These observations suggest ultrafast STA play a critical role in the optical gain processes.

According to the transient PL spectra in Figure 3d, the emission on the $\langle n \rangle = 8$ domains in the absence of oxygen already shows ~50% quenching at 250 fs, close to the limit of our time-resolution, indicating the significant impact of STA on the thick Q2D domains. However, the emission intensity on the ultrathin $\langle n \rangle = 2$ domains is less affected, with similar signal intensities within the first 300 fs and confirmed by their kinetic evolution in the presence and absence of oxygen (see SI Figure S6). This shows that STA directly competes with energy funnelling. While oxygen in the environment prevents the accumulation of long-lived triplet states, excitons generated on ultrathin grains can rapidly transfer their energy down to the thicker grains with a smaller bandgap. On the other hand, the accumulation of triplet states on the thin highly excitonic domains in the absence of oxygen followed

by the annihilation of the bright singlet state population before energy transfer is finished is evidence of ultrafast, highly-efficient quenching behaviour on the ASE site [55].

Since we found dynamic quenching behaviour on the ultrathin highly excitonic grains, we can use an STA model (see SI for details) to describe the underlying kinetics of the bright singlet excitons and obtain quantitative values associated with the bimolecular recombination constant of the STA annihilation process by analysing the repetition rate dependent PL kinetics (see SI for details). We obtain an STA rate of γ_{ST} = $6.0 \cdot 10^{-7}$ $cm^3 s^{-1}$ within the <*n*> = 2 grains, which is comparable with the STA rates reported for organic semiconductors [43,55–57] and is one order of magnitude faster than the extracted rate for singlet-singlet exciton annihilation (SSA) (see SI Figure S8). Moreover, the STA rate we obtain is likely underestimated by up to one order of magnitude in order to account for the ~50% of quenching we observe within the 250-fs instrument response. The effects of different assumptions on limiting values of the STA rate are modelled in the SI (Figure S10). Our experimental results confirm that STA comprising energy funnelling between the nanoplates is the dominant process for the absence of ASE.

Discussion

We reveal the picosecond formation of ASE, showing that photoexcitations can be efficiently harvested to the emission sites to achieve population inversion. The decrease in the energy band gap with the increase in the number of layers of the nanoplate provides an efficient route for the cascading transfer of energy.[58] Our observation highlights the significance of similar time scales in ASE and energy funnelling dynamics, revealing the essential role of efficient energy transfer from high-confinement nanoplates to the lasing sites. This mechanism, which involves redistributing photoexcitation, significantly enhances the lasing processes in Q2D PVSK (Scheme A). Previously, the energy-funnelling dynamics had been revealed by transient absorption spectroscopy in Q2D PVSK.[16,59] However, TA faces a significant challenge in this task due to the complexity of mixed-layer materials, which results in overlapping spectral signatures when short-wavelength excitation simultaneously

excites all plate sizes. Additionally, since previous experiments were conducted under non-lasing conditions, the resolved dynamics may not accurately reflect or be directly linked to lasing action. We further utilize the generalized Förster Resonance Energy Transfer (FRET) formalism to calculate the rate of energy transfer between Q2D layers possessing distinct <*n*> values within the Q2D perovskite film. Detailed analysis is available in the supporting information. Notably, the estimated transfer rates are significantly slower, specifically two orders of magnitude less, compared to the sub-picosecond funnelling timescale observed in our ultrafast photoluminescence spectroscopy studies. This mismatch in time scales strongly suggests that the energy funnelling process happens faster than the exciton-phonon relaxation time in each individual Q2D layers, since FRET assumes the opposite. This hypothesis is further bolstered by the established presence of slow hot carrier relaxation in perovskites, often due to mechanisms like the hot-phonon bottleneck. Other possible sources of error include the variation of inter-layer distances (scales as d^{-4}), the estimation of average exciton sizes ($A = a^2$), as well as the possibility of non-dipole contribution to the excitonic coupling ($a > d$). These factors require further microscopic details that are unavailable and beyond the current study.

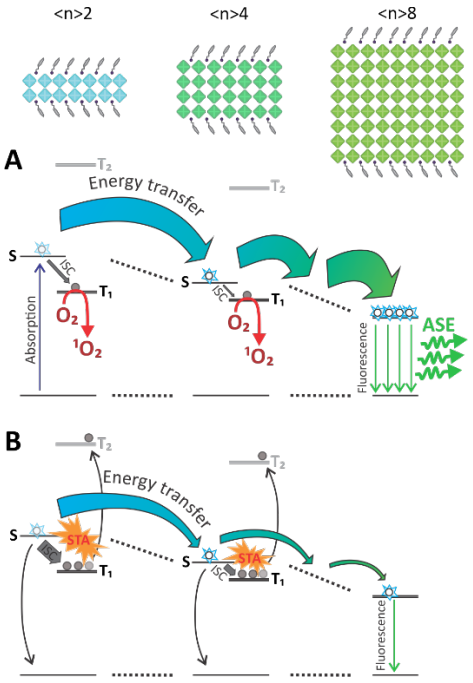

Figure 4: (A) Schematic illustration of cascade energy transfer from wide to small band gap domains in mixed Q2D perovskite films in the presence of oxygen which acts as a triplet state quencher. (B) Accumulation of long-lived triplet states on highly

confined domains in the absence of oxygen introduces a competing singlet-triplet annihilation channel for the bright singlet state population.

As the PL quenching of STA was only observed at 343 nm but not at 515 nm excitation conditions, we can conclude that STA is linked to energy funnelling. Indeed, at 343 nm excitation, the short-lived PL signals from $2 \leq \langle n \rangle \leq 5$ provide the evidence of picosecond energy funnelling. Moreover, the evidence of ultrafast (<200 fs) STA gives us a temporal reference to estimate the energy funnelling in sub-ps time scales. Based on this picture and the 50% PL quenching of ASE sites by STA within 200 fs, we can conclude that when STA is deactivated in an oxygen containing environment, about 50% of the initial excitation on $\langle n \rangle$=8 plates is from the thinner plates by energy funnelling. This ultrafast energy funnelling can originate from the close-packing of the Q2D plates, good spectral overlap between the donor and acceptor, and coupling between high dimension donor-acceptor systems beyond the Förster resonance energy transfer regime.[60,61]

Next, we consider the impact of STA. Although the efficient energy transfer on sub-picosecond timescales benefits the Q2D PVSK lasing process, our experimental results show that the energy transfer cascade is quickly outcompeted by STA at high excitation densities. This observation can explain the enormous consequences of STA for the optical performance of Q2D perovskites under current injection and CW excitation. The critical ultrafast exciton dynamics during the lasing process resolved here is related to the Q2D PVSK nature of the mixture of strong and weak excitonic characters of the nanoplates. As the exchange energy increases with increasing confinement, the triplet excitons are more stable in the thin, high confinement nanoplates. Moreover, considering that the energy transfer of triplet excitons is an electron-exchange mediated process with a short interaction distance, the organic spacers at the grain boundaries likely prevent the transfer of dark excitons between individual slabs [62,63] and confine them within the thin $\langle n \rangle$ grains. The results of this study show that the effective accumulation of triplet states, in agreement with the effect of triplet accumulation proposed by Qin, depends on the excitonic character of the Q2D perovskite slabs, and that a fraction

of strongly confined grains within a mixed Q2D film has a profound limiting effect on the overall emission and optical gain properties.

In Figure 4, we propose the scheme of the lasing dynamics of Q2D PVSK involving energy funnelling and STA. The initial photoexcitation in the thin nanoplate can employ rapid cascade energy transfer to the lasing site; however, as the triplet excitons accumulate in the other high-confinement nanoplate, the efficient energy funnelling also increases the opportunity for singlet-triplet exciton interactions before the excitations reach the <*n*>=8 nanoplate. However, excitation species generated in weakly confined grains are inherently free charge carriers and do not accumulate for two reasons: their low exciton binding energy supports thermally activated exciton dissociation, and the small singlet-triplet energy spacing (several meVs [63]) leads to fast RISC.

The results of this study show that the effective accumulation of triplet states and their interference with ultrafast energy funnelling has a profound limiting effect on the overall emission and optical gain properties. This interplay explains the absence of triplet interactions in the study by Li *et al.* [4640] because in spite of exciting excitonic grains at 405 nm, the 260 fs excitation pulses used are too short for singlet-triplet interactions within the pulse, and the low laser repetition rate (1 kHz) gave the triplet excitons sufficient time to decay before the next pulse. On the other hand, the observation of STA by Qin *et al.* [5] can be attributed to the nanosecond pump length (3 ns, 337 nm, 20 kHz), which appears to lead to the accumulation of triplets during excitation. This accumulation is likely the result of intersystem crossing between states which occurs within picoseconds [37], annihilating newly generated bright states via STA while the laser pulse is still passing through the film.

Under elevated excitation densities, the energy transfer cascade is rapidly surpassed by singlet-triplet annihilation (STA), which has significant implications for the optical performance of quasi-two-dimensional (Q2D) perovskites under continuous-wave (CW) excitation and current injection. Our findings align with Qin et al.'s research, which suggests managing triplets through the use of organic ligands to extract dark excitons from the perovskite matrix. Additionally, our study emphasises the

crucial role of the energy landscape in exciton dynamics. We have successfully resolved excitations traversing distinct energy landscapes by employing time-resolved emission spectroscopy and manipulating experimental parameters, such as excitation wavelength and repetition rate. Given that the energy landscape in Q2D perovskites arises from variations in layer thickness, our research highlights the importance of controlling both the excitation wavelength and size distribution of Q2D perovskites for lasing applications.

Conclusion

This study comprehensively investigates the ultrafast photoexcitation dynamics in Q2D PVSK. Our results demonstrate the rapid build-up of ASE in Q2D PVSK within picoseconds, indicating efficient population inversion and high potential for laser material applications. Moreover, the efficient energy funnelling process reveals Q2D PVSK thin film are an excellent energy harvesting system. However, the ultrafast STA and the accumulation of triplet excitons serve as dominant quenching processes, which limits its overall performance. By clarifying the relationship between the critical ultrafast mechanisms and lasing action in Q2D PVSK, we highlight the importance of monodispersion and pumping wavelength for Q2D PVSK lasing application through a fundamental understanding. These findings provide important insights into the design and optimisation of Q2D perovskites for optoelectronic applications.

Methods

Transient grating photoluminescence spectroscopy

For the detection of the broadband PL transients on a sub-picosecond timescale, we used a transient grating PL technique [50]. The output of a femtosecond Ytterbium fiber laser (Tangerine SP, Amplitude Systemes; <150 fs) was split into pump and gate parts. For the pump part, second harmonic (515 nm) and third harmonic (343 nm) generations were used in the experiments and were focused on a 70 μm^2 spot on the sample. During the measurement, the perovskite films were kept inside an airtight sample holder and either vacuum conditions were applied to simulate a triplet quencher free environment, or a flood of ambient air was provided to introduce oxygen. The PL signal from the sample was collected and refocused onto the gate medium (1 mm fused silica crystal) using a pair of off-axis parabolic mirrors. For the gate part, about 40 µJ 1030 nm output was split using a 50/50 beam splitter to generate the two gate beams which were focused onto the gate medium at a crossing angle of approximately 8° and overlapped with the PL in a BOXCAR geometry. Due to the spatial and temporal overlap inside the gate medium, the two gate beams generate a laser-induced grating. The transient grating acts like an ultrafast optical shutter to temporally resolve the broadband PL signals by diffracting the gated signal from the PL background. An off-axis parabolic mirror and an achromatic lens was used to collimate and focus the gated signals onto the spectrometer entrance (Princeton Instruments SP 2300), respectively. The gated PL spectra were measured by an intensified CCD camera (Princeton Instruments, PIMAX3). A 380 nm or 550 nm long- and 850 nm short-pass filter were used to remove the residual pump and intense 1030 nm gate, respectively. The time delay between pump and gate beams was controlled via a motorized optical delay line. For the repetition rate dependent experiments, the integrated pulse picker within the amplifier unit has been used to change the laser repetition rate without effecting the output pulse energy. For the fluence dependent steady state photoluminescence spectrum and time-resolved decay dynamics on a microsecond timescale, the SP 2300 spectrometer and PIMAX 3 ICCD were used to record the steady state emission spectra.

Acknowledgements

I.W and K. C. acknowledge support from the Marsden Fund (17-VUW-154), Royal Society of New Zealand. W.T.M.V.G., L.L., P.G. and D.V. acknowledge the FWO for the funding of the SBO project PROCEED (FWOS002019N) and the senior FWO research project G043320N. The authors thank Bart Ruttens (imo-imomec) for XRD measurements.

Author information

Authors and Affiliations

MacDiarmid Institute for Advanced Materials and Nanotechnology, and School of Chemical and Physical Sciences, Victoria University of Wellington, 6012, Wellington, New Zealand.

Isabella Wagner, Paul A. Hume, Michael B. Price, and Justin M. Hodgkiss

Hybrid Materials Design (HyMaD), Institute for Materials Research (IMO), Hasselt University, 3500, Hasselt, Belgium

Wouter T.M. Van Gompel, Laurence Lutsen and Dirk Vanderzande

Associated Laboratory IMOMEC, Imec, 3590, Diepenbeek, Belgium

Laurence Lutsen and Dirk Vanderzande

Department of Chemistry and Biochemistry, University of Nevada, Las Vegas, Nevada 89154, United States

Chern Chuang

Department of Physics, Chung Yuan Christian University, 320314, Taoyuan, Taiwan

Sheng Hsiung Chang

Center for Nano and Biophotonics, and Physics and Chemistry of Nanostructures, Ghent University, 9000, Ghent, Belgium

Pieter Geiregat

The Dodd-Walls Centre for Photonic and Quantum Technologies, Dunedin, New Zealand, and MacDiarmid Institute for Advanced Materials and Nanotechnology, and Robinson Research Institute, Victoria University of Wellington, 6012, Wellington, New Zealand

Kai Chen

Contributions

I.W., P.G. and K.C. conceived of the experiments. J.M.H. and K.C. supervised the project. K.C. designed and built the ultrafast PL system. I.W. carried out the spectroscopic measurements, analysed and modelled the data. W.T.M.V.G. synthesized and characterized the Q2D perovskite films. C.C. performed the generalized Förster Resonance Energy Transfer analysis. S.H.C. prepared the MAPbI3 perovskite film. I.W., J.M.H. and K.C. wrote the manuscript. All authors contributed to the discussion of the results and commented on the manuscript.

References

1. Snaith, H. J. Perovskites. The Emergence of a New Era for Low-Cost, High-Efficiency Solar Cells. *Journal of Physical Chemistry Letters* **4,** 3623–3630; 10.1021/JZ4020162 (2013).
2. Wehrenfennig, C., Eperon, G. E., Johnston, M. B., Snaith, H. J. & Herz, L. M. High charge carrier mobilities and lifetimes in organolead trihalide perovskites. *Advanced Materials* **26,** 1584–1589; 10.1002/adma.201305172 (2014).
3. Wang, N. *et al.* Perovskite light-emitting diodes based on solution-processed self-organized multiple quantum wells. *Nature Photonics* **10,** 699–704; 10.1038/nphoton.2016.185 (2016).
4. Lin, K. *et al.* Perovskite light-emitting diodes with external quantum efficiency exceeding 20 percent. *Nature* **562,** 245–248; 10.1038/s41586-018-0575-3 (2018).
5. Qin, C. *et al.* Stable room-temperature continuous-wave lasing in quasi-2D perovskite films. *Nature* **585,** 53–57; 10.1038/s41586-020-2621-1 (2020).
6. Zhao, C. & Qin, C. Quasi-2D lead halide perovskite gain materials toward electrical pumping laser. *Nanophotonics* **10,** 2167–2180; 10.1515/NANOPH-2020-0630 (2020).
7. Wolf, S. de *et al.* Organometallic halide perovskites. Sharp optical absorption edge and its relation to photovoltaic performance. *Journal of Physical Chemistry Letters* **5,** 1035–1039; 10.1021/jz500279b (2014).
8. Deschler, F. *et al.* High photoluminescence efficiency and optically pumped lasing in solution-processed mixed halide perovskite semiconductors. *Journal of Physical Chemistry Letters* **5,** 1421–1426; 10.1021/jz5005285 (2014).
9. Stranks, S. D. *et al.* Electron-hole diffusion lengths exceeding 1 micrometer in an organometal trihalide perovskite absorber. *Science* **342,** 341–344; 10.1126/science.1243982 (2013).
10. Xing, G. *et al.* Long-range balanced electron-and hole-transport lengths in organic-inorganic CH3NH3PbI3. *Science* **342,** 344–347; 10.1126/science.1243167 (2013).
11. Eperon, G. E. *et al.* Formamidinium lead trihalide. A broadly tunable perovskite for efficient planar heterojunction solar cells. *Energy & Environmental Science* **7,** 982–988; 10.1039/C3EE43822H (2014).

12. Filip, M. R., Eperon, G. E., Snaith, H. J. & Giustino, F. Steric engineering of metal-halide perovskites with tunable optical band gaps. *Nature Communications* **5,** 1–9; 10.1038/ncomms6757 (2014).

13. Zhang, X. *et al.* Quasi-CW Amplified Spontaneous Emission in Air-Processed Quasi-2D Perovskite Thin Films with High Stability. *Adv Funct Materials* **34**; 10.1002/adfm.202315172 (2024).

14. Lee, G., Jun, Y., Lee, H. & Roh, K. Progress on Coherent Perovskites Emitters. From Light-Emitting Diodes under High Current Density Operation to Laser Diodes. *Advanced Photonics Research* **5**; 10.1002/adpr.202400033 (2024).

15. Jiang, X. *et al.* Mixing Dion–Jacobson and Ruddlesden–Popper Structures in Quasi-2D Perovskite Films for Thermal- and Photo-Stable Stimulated Emission. *Advanced Optical Materials* **11,** 115; 10.1002/adom.202300806 (2023).

16. Yuan, M. *et al.* Perovskite energy funnels for efficient light-emitting diodes. *Nature Nanotechnology* **11,** 872–877; 10.1038/nnano.2016.110 (2016).

17. Jia, G. *et al.* Super air stable quasi-2D organic-inorganic hybrid perovskites for visible light-emitting diodes. *Optics Express* **26,** A66; 10.1364/oe.26.000a66 (2018).

18. Smith, I. C., Hoke, E. T., Solis-Ibarra, D., McGehee, M. D. & Karunadasa, H. I. A Layered Hybrid Perovskite Solar-Cell Absorber with Enhanced Moisture Stability. *Angewandte Chemie* **126,** 11414–11417; 10.1002/ange.201406466 (2014).

19. Herckens, R. *et al.* Multi-layered hybrid perovskites templated with carbazole derivatives. Optical properties, enhanced moisture stability and solar cell characteristics. *Journal of Materials Chemistry A* **6,** 22899–22908; 10.1039/c8ta08019d (2018).

20. van Gompel, W. T.M. *et al.* 2D layered perovskite containing functionalised benzothieno-benzothiophene molecules. Formation, degradation, optical properties and photoconductivity. *Journal of Materials Chemistry C* **8,** 7181–7188; 10.1039/d0tc01053g (2020).

21. Chakraborty, R. & Nag, A. Correlation of Dielectric Confinement and Excitonic Binding Energy in 2D Layered Hybrid Perovskites Using Temperature Dependent Photoluminescence. *J. Phys. Chem. C* **124,** 16177–16185; 10.1021/acs.jpcc.0c04284 (2020).

22. Ishihara, T., Hong, X., Ding, J. & Nurmikko, V. A. Dielectric confinement effect for exciton and biexciton states in PbI4-based two-dimensional semiconductor structures. *Surface Science* **267,** 323–326; 10.1016/0039-6028(92)91147-4 (1992).

23. Huang, S. *et al.* Enhanced Amplified Spontaneous Emission in Quasi-2D Perovskite by Facilitating Energy Transfer. *ACS Appl. Mater. Interfaces* **14,** 33842–33849; 10.1021/acsami.2c07633 (2022).

24. Cho, H. *et al.* Overcoming the electroluminescence efficiency limitations of perovskite light-emitting diodes. *Science* **350,** 1222–1225; 10.1126/science.aad1818 (2015).

25. Fakharuddin, A. *et al.* Reduced Efficiency Roll-Off and Improved Stability of Mixed 2D/3D Perovskite Light Emitting Diodes by Balancing Charge Injection. *Advanced Functional Materials* **29,** 1904101; 10.1002/ADFM.201904101 (2019).

26. Zou, C., Liu, Y., Ginger, D. S. & Lin, L. Y. Suppressing Efficiency Roll-Off at High Current Densities for Ultra-Bright Green Perovskite Light-Emitting Diodes. *ACS Nano* **14,** 6076–6086; 10.1021/ACSNANO.0C01817/ASSET/IMAGES/LARGE/NN0C01817_0005.JPEG (2020).

27. Zou, D. *et al.* Low-Threshold Amplified Spontaneous Emission from Defect-Passivated Quasi-2D Perovskites. *J. Phys. Chem. C* **127,** 21841–21848; 10.1021/acs.jpcc.3c05840 (2023).

28. Li, M. *et al.* Amplified Spontaneous Emission Based on 2D Ruddlesden–Popper Perovskites. *Advanced Functional Materials* **28,** 1707006; 10.1002/ADFM.201707006 (2018).

29. Zhang, H. *et al.* 2D Ruddlesden–Popper Perovskites Microring Laser Array. *Advanced Materials* **30,** 1706186; 10.1002/ADMA.201706186 (2018).

30. Gu, L. *et al.* High Q-Factor and Low Threshold Continuous-Wave Near-Infrared Lasing with Quasi-2D Perovskites. *Adv Funct Materials* **33**; 10.1002/adfm.202303900 (2023).

31. Banin, U., Lee, J. C., Guzelian, A. A., Kadavanich, V. A. & Alivisatos, A. P. Exchange interaction in InAs nanocrystal quantum dots. *Superlattices and Microstructures* **22,** 559–568; 10.1006/spmi.1997.0504 (1997).

32. Calcott, P. D.J., Nash, K. J., Canham, L. T., Kane, M. J. & Brumhead, D. Identification of radiative transitions in highly porous silicon. *Journal of Physics: Condensed Matter* **5,** L91; 10.1088/0953-8984/5/7/003 (1993).

33. Chamarro, M., Gourdon, C., Lavallard, P., Lublinskaya, O. & Ekimov, A. Enhancement of electron-hole exchange interaction in CdSe nanocrystals. A quantum confinement effect. *Physical Review B - Condensed Matter and Materials Physics* **53,** 1336–1342; 10.1103/PhysRevB.53.1336 (1996).

34. Fang, H. H. *et al.* Band-Edge Exciton Fine Structure and Exciton Recombination Dynamics in Single Crystals of Layered Hybrid Perovskites. *Advanced Functional Materials* **30,** 1907979; 10.1002/adfm.201907979 (2020).

35. Do, T. T. H. *et al.* Bright Exciton Fine-Structure in Two-Dimensional Lead Halide Perovskites. *Nano Letters* **20,** 5141–5148; 10.1021/acs.nanolett.0c01364 (2020).

36. Folpini, G., Cortecchia, D., Petrozza, A. & Srimath Kandada, A. R. The role of a dark exciton reservoir in the luminescence efficiency of two-dimensional tin iodide perovskites. *Journal of Materials Chemistry C* **8,** 10889–10896; 10.1039/d0tc01218a (2020).

37. Ema, K., Inomata, M., Kato, Y., Kunugita, H. & Era, M. Nearly perfect triplet-triplet energy transfer from wannier excitons to naphthalene in organic-inorganic hybrid quantum-well materials. *Physical Review Letters* **100,** 257401; 10.1103/PhysRevLett.100.257401 (2008).

38. Tanaka, K. *et al.* Electronic and excitonic structures of inorganic-organic perovskite-type quantum-well crystal (C4H9NH3) 2PbBr4. *Japanese Journal of Applied Physics* **44,** 5923–5932; 10.1143/JJAP.44.5923 (2005).

39. Tamaki, R. *et al.* Exciton polariton in an organic-inorganic multiple-quantum-well crystal (C4H9NH3)2PbBr4. *Journal of Luminescence* **128,** 842–844; 10.1016/j.jlumin.2007.11.061 (2008).

40. Younts, R. *et al.* Efficient Generation of Long-Lived Triplet Excitons in 2D Hybrid Perovskite. *Advanced Materials* **29,** 1604278; 10.1002/adma.201604278 (2017).

41. Ema, K. *et al.* Huge exchange energy and fine structure of excitons in an organic-inorganic quantum well material. *Physical Review B* **73,** 241310; 10.1103/PhysRevB.73.241310 (2006).

42. Giebink, N. C. & Forrest, S. R. Temporal response of optically pumped organic semiconductor lasers and its implication for reaching threshold under electrical excitation. *Physical Review B* **79,** 73302; 10.1103/PhysRevB.79.073302 (2009).

43. Lehnhardt, M., Riedl, T., Weimann, T. & Kowalsky, W. Impact of triplet absorption and triplet-singlet annihilation on the dynamics of optically pumped organic solid-state lasers. *Physical Review B* **81,** 165206; 10.1103/PhysRevB.81.165206 (2010).

44. Inoue, M., Matsushima, T., Nakanotani, H. & Adachi, C. Introduction of oxygen into organic thin films with the aim of suppressing singlet–triplet annihilation. *Chemical Physics Letters* **624,** 43–46; 10.1016/J.CPLETT.2015.02.010 (2015).

45. Qin, C. *et al.* Triplet management for efficient perovskite light-emitting diodes. *Nature Photonics* **14,** 70–75; 10.1038/s41566-019-0545-9 (2020).

46. Li, Y. *et al.* Exciton versus free carrier emission. Implications for photoluminescence efficiency and amplified spontaneous emission thresholds in quasi-2D and 3D perovskites. *Materials Today* **49,** 35–47; 10.1016/j.mattod.2021.05.002 (2021).

47. Hu, H. *et al.* Efficient Room-Temperature Phosphorescence from Organic–Inorganic Hybrid Perovskites by Molecular Engineering. *Advanced Materials* **30,** 1707621; 10.1002/adma.201707621 (2018).

48. Gan, Z. *et al.* Transient Energy Reservoir in 2D Perovskites. *Advanced Optical Materials* **7,** 1900971; 10.1002/ADOM.201900971 (2019).

49. Fujiwara, K. *et al.* Excitation Dynamics in Layered Lead Halide Perovskite Crystal Slabs and Microcavities. *ACS Photonics* **7,** 845–852; 10.1021/ACSPHOTONICS.0C00038 (2020).

50. Chen, K., Gallaher, J. K., Barker, A. J. & Hodgkiss, J. M. Transient grating photoluminescence spectroscopy. An ultrafast method of gating broadband spectra. *Journal of Physical Chemistry Letters* **5,** 1732–1737; 10.1021/jz5006362 (2014).

51. Yu, M. *et al.* Control of Barrier Width in Perovskite Multiple Quantum Wells for High Performance Green Light–Emitting Diodes. *Advanced Optical Materials* **7,** 1801575; 10.1002/ADOM.201801575 (2019).

52. Stoumpos, C. C. *et al.* Ruddlesden-Popper Hybrid Lead Iodide Perovskite 2D Homologous Semiconductors. *Chemistry of Materials* **28,** 2852–2867; 10.1021/acs.chemmater.6b00847 (2016).

53. Meckler, A. Electronic energy levels of molecular oxygen. *The Journal of Chemical Physics* **21,** 1750–1762; 10.1063/1.1698657 (1953).

54. Zhu, Y. *et al.* Self-Assembled Ruddlesden–Popper/Perovskite Hybrid with Lattice-Oxygen Activation as a Superior Oxygen Evolution Electrocatalyst. *Small* **16,** 2001204; 10.1002/smll.202001204 (2020).

55. Hofkens, J. *et al.* Revealing competitive Förster-type resonance energy-transfer pathways in single bichromophoric molecules. *Proceedings of the National Academy of Sciences of the United States of America* **100,** 13146–13151; 10.1073/pnas.2235805100 (2003).

56. List, E. J.W. *et al.* Direct evidence for singlet-triplet exciton annihilation in π-conjugated polymers. *Physical Review B - Condensed Matter and Materials Physics* **66,** 1–5; 10.1103/PhysRevB.66.235203 (2002).

57. Zaushitsyn, Y., Jespersen, K. G., Valkunas, L., Sundström, V. & Yartsev, A. Ultrafast dynamics of singlet-singlet and singlet-triplet exciton annihilation in poly(3- 2´ -methoxy- 5´ octylphenyl)thiophene films. *Physical Review B* **75,** 195201; 10.1103/PhysRevB.75.195201 (2007).

58. Jiang, Y., Wei, J. & Yuan, M. Energy-Funneling Process in Quasi-2D Perovskite Light-Emitting Diodes. *The journal of physical chemistry letters* **12,** 2593–2606; 10.1021/acs.jpclett.1c00072 (2021).

59. Zhang, H. *et al.* A Two-Dimensional Ruddlesden-Popper Perovskite Nanowire Laser Array based on Ultrafast Light-Harvesting Quantum Wells. *Angewandte Chemie (International ed. in English)* **57,** 7748–7752; 10.1002/anie.201802515 (2018).

60. Algar, W. R., Kim, H., Medintz, I. L. & Hildebrandt, N. Emerging non-traditional Förster resonance energy transfer configurations with semiconductor quantum dots. Investigations and applications. *Coordination Chemistry Reviews* **263-264,** 65–85; 10.1016/j.ccr.2013.07.015 (2014).

61. Andrews, D. L., Curutchet, C. & Scholes, G. D. Resonance energy transfer. Beyond the limits. *Laser & Photon. Rev.* **5,** 114–123; 10.1002/lpor.201000004 (2011).

62. Lee, D. S. *et al.* Passivation of Grain Boundaries by Phenethylammonium in Formamidinium-Methylammonium Lead Halide Perovskite Solar Cells. *ACS Energy Letters* **3,** 647–654; 10.1021/acsenergylett.8b00121 (2018).

63. Gramlich, M. *et al.* Dark and Bright Excitons in Halide Perovskite Nanoplatelets. *Advanced Science* **9,** 2103013; 10.1002/advs.202103013 (2021).